A Systematic Computational Methodology Applied to a Three-Dimensional Film-Cooling Flowfield

D. K. Walters

J. H. Leylek

Department of Mechanical Engineering,
Clemson University,
Clemson, SC 29632

Numerical results are presented for a three-dimensional discrete-jet in crossflow problem typical of a realistic film-cooling application in gas turbines. Key aspects of the study include: (1) application of a systematic computational methodology that stresses accurate computational model of the physical problem, including simultaneous, fully elliptic solution of the crossflow, film-hole, and plenum regions; high-quality three-dimensional unstructured grid generation techniques, which have yet to be documented for this class of problems; the use of a high-order discretization scheme to reduce numerical errors significantly; and effective turbulence modeling; (2) a three-way comparison of results to both code validation quality experimental data and a previously documented structured grid simulation; and (3) identification of sources of discrepancy between predicted and measured results, as well as recommendations to alleviate these discrepancies. Solutions were obtained with a multiblock, unstructured/adaptive grid, fully explicit, time-marching, Reynolds-averaged Navier–Stokes code with multigrid, local time stepping, and residual smoothing type acceleration techniques. The computational methodology was applied to the validation test case of a row of discrete jets on a flat plate with a streamwise injection angle of 35 deg, and two film-hole length-to-diameter ratios of 3.5 and 1.75. The density ratio for all cases was 2.0, blowing ratio was varied from 0.5 to 2.0, and free-stream turbulence intensity was 2 percent. The results demonstrate that the prescribed computational methodology yields consistently more accurate solutions for this class of problems than previous attempts published in the open literature. Sources of disagreement between measured and computed results have been identified, and recommendations made for future prediction of film-cooling problems.

1 Introduction

Film cooling is commonly used in the gas turbine industry to prevent hot-section components from failing at elevated temperatures. Increasingly, designers are trying to extract greater cooling performance from less coolant air, particularly in next-generation high-efficiency gas turbines. To make significant advances in cooling technology requires a fundamental understanding of the physical mechanisms involved in film-cooling flowfields. At the same time, designers need a truly predictive design tool that allows relatively quick turnaround times without the "build 'em and bust 'em" approach that is currently used. Computational fluid dynamics presents the designer with the potential for an effective, fast, and accurate method of achieving these goals.

Most computational work for film-cooling problems has focused on the interaction of a three-dimensional discrete jet with a crossflow. It is exactly this problem that is at the heart of film-cooling physics. Unfortunately, the majority of past attempts to simulate this class of problems have suffered in one or more critical areas, resulting in solutions that have been inaccurate and, more importantly, inconsistent. This paper presents the results from a series of simulations based on a systematic approach to the four critical issues of a computational simulation. These are: (1) proper computational modeling of flow physics; (2) exact geometry and high-quality grid generation; (3)

higher-order discretization scheme; and (4) effective turbulence modeling. By addressing each of the first three issues in a systematic manner, the present simulations allow a true judgment to be made regarding turbulence model performance for film-cooling problems. It is shown that adherence to the prescribed methodology results in a more consistently accurate computational procedure than any documented in the open literature to date.

2 Literature Review

The interaction of jets-in-crossflow has been heavily researched. The following review examines the more relevant studies that have been documented for three-dimensional jets, both experimental and computational.

2.1 Experimental Studies. Bergeles et al. (1976, 1977) documented early investigations of a single discrete jet injected into a crossflow, both normally (1976) and at a 30 deg streamwise injection angle (1977). The authors documented the variation in jet lift-off and penetration as blowing ratio increased along with the entrainment of the mainstream fluid into the separation region beneath the jet. They also identified the non-uniformity of the jet exit profile, suggesting the influence of the crossflow on the flow within the film-hole.

Andreopoulos and Rodi (1984) documented an extensive experimental study of an isolated normal jet-in-crossflow, showing the counterrotating vortex structure within the jet as the jet interacted with the crossflow and the presence of a "blockage" over the upstream portion of the coolant jet exit plane. They noted that the amount of blockage varied with blowing ratio,

suggesting an influence by the crossflow on the flow within the film hole. The authors concluded that eddy-viscosity turbulence models should be capable of accurately prescribing two of the three Reynolds stress quantities, the exception being the term influencing the lateral spreading of the coolant jet.

Pietrzyk et al. (1988, 1990) and Sinha et al. (1991) made significant advances in the experimental modeling of film-cooling flowfields. They studied the hydrodynamic and thermal characteristics of a row of discrete jets inclined at 35 deg to the crossflow with a short film-hole length-to-diameter (L/D) ratio. Detailed mean flow and turbulence quantities were presented throughout the flowfield, as well as surface measurements of adiabatic film effectiveness. The authors hypothesized the existence of a separation region within the film-hole itself as they attempted to explain the shape of the velocity profiles and high turbulence intensities measured at the exit plane of the film-hole. The results suggested that the presence of the supply plenum and the length of the film hole were important factors in determining the flowfield characteristics. They also found a direct correlation between the peaks in the mean velocity gradients and the peaks in turbulence shear stresses along the jet centerline, concluding that an eddy-viscosity turbulence model would be adequate in this region.

2.2 Computational Studies.
Bergeles et al. (1978) supplemented their experimental study with a numerical treatment for normal and 30 deg inclined round jets. They used a "partially parabolic" scheme in which pressure information was allowed to propagate upstream and all other flow variables were treated using a fully parabolic space-marching procedure. Initially, the authors believed that the near-field character of the jet was insensitive to the jet exit profile. Based on this assumption, they imposed a uniform jet exit profile as a boundary condition on the crossflow. The simulation used an extremely coarse grid (5415 cells) in combination with a low-order discretization scheme. Turbulence quantities were obtained using a primitive anisotropic mixing length turbulence model. The results indicated that a fully elliptic solution procedure was needed to capture the near-field character of the jet accurately, especially in those cases where a separation region appeared downstream of the film hole. The authors also found that their assumption of insensitivity to jet exit profile was valid only for cases with blowing ratio less than 0.2. At more realistic blowing ratios, they suggested that the computational domain be extended into the film hole. Finally, the simulations demonstrated the anisotropic nature of the turbulent stresses, and the authors suggested the use of an algebraic Reynolds stress model in favor of the more conventional eddy-viscosity turbulence models.

Demuren (1982) performed a series of simulations for a row of discrete jets issuing normally into a crossflow, concentrating on the effects of grid refinement and discretization scheme on the overall solution. The results showed that for any grid level, the QUICK scheme (Leonard, 1979) introduced less numerical viscosity and gave superior solutions to the lower-order hybrid scheme (Patankar, 1980). However, the simulation domain used the typical practice of modeling only the crossflow region, introducing the jet as a uniform total pressure boundary condition with the exit plane geometry approximated as a right-angled polygon of equal area. The author noted the sensitivity of the

solution to the jet exit boundary conditions, but ascribed deviations between predicted and measured data to the isotropic nature of the $k-\epsilon$ turbulence model.

Leylek and Zerkle (1994) were the first to perform a jet-in-crossflow simulation using a geometry typical of that found in film-cooling applications. The primary objective of their study was to develop a proper computational model of the gas turbine film-cooling flowfield. Their simulations were based on the experimental work of Pietrzyk et al. (1988, 1990) and Sinha et al. (1991) described above. The computational domain included not only the crossflow, but also the film-hole and supply plenum regions, with short film-hole length-to-diameter ratios of 3.5 and 1.75. Solving these regions simultaneously, the authors noted the strong three-way coupling between the plenum, film-hole, and crossflow regions. They identified a very complex flow structure within the film hole, which caused the jet exit conditions to change dramatically as blowing ratio varied. Unfortunately, the single-block structured grid procedure presented serious difficulties in maintaining a refined, high-quality grid in the jet exit region. The simulation also used a lower-order discretization scheme (hybrid), which resulted in increased numerical errors.

One of the earliest unstructured/adaptive simulations for this class of problems was documented by Weigand and Harasgama (1994). The study used the unstructured/adaptive code developed by Dawes (1991) on an entire turbine blade with multiple jet injection and rotation effects. Due to the large domain, the solution used an extremely coarse grid relative to the jet size, and gridding limitations forced the authors to model the injection holes along blade-to-blade grid lines. The study did not attempt to document the details of the jet–crossflow interaction, so unfortunately the performance of the unstructured/adaptive procedure could not be evaluated in this regard.

Recently, Garg and Gaugler (1997) demonstrated the importance of the jet exit plane conditions on downstream results. The authors performed simulations for three different blade configurations using $\frac{1}{7}$th power-law and "tuned" polynomial jet exit profiles for velocity and temperature distribution. The results showed that downstream heat transfer coefficient levels may differ by as much as 60 percent depending on the exit profile used, highlighting the critical influence of the jet exit conditions on downstream results.

2.3 Summary.
The papers cited above show that the interaction between jet and crossflow is not confined to the crossflow region alone. Each study describes the profile variations at the jet exit plane as the operating conditions change. They also show that as the geometry of the experimental model more closely matches the small L/D geometries used in gas turbine film-cooling applications, the variation in exit profiles is even more significant. Particularly, for cases that use realistic L/D ratios, the flowfield exhibits a three-way coupling behavior between the crossflow, film-hole, and plenum regions. Despite this well-documented, complex behavior, computational simulations continue to apply boundary conditions at either the jet exit plane or the film-hole inlet. In addition, most documented computational treatments suffer from inadequate geometry and grid generation procedures, which do not allow a high-quality, refined grid to be maintained in the critical regions of the flow-

---

Nomenclature

D = film-hole diameter
DR = density ratio = ϱ_j/ϱ_∞
L/D = film-hole length-to-diameter ratio
M = blowing (or mass flux) ratio = $\varrho_j v_j/\varrho_\infty u_\infty$
T_j = coolant jet temperature
T_w = wall temperature

T_∞ = mainstream temperature
TKE = turbulence kinetic energy
u_∞ = mainstream velocity
v_j = jet exit velocity
x = streamwise coordinate
y^+ = nondimensional distance from wall

z = lateral coordinate
η = adiabatic effectiveness = $(T_\infty - T_{aw})/(T_\infty - T_j)$
$\bar{\eta}$ = laterally averaged adiabatic effectiveness
ϱ_j = coolant density
ϱ_∞ = mainstream density

field. Many simulations also suffer from the use of lower-order discretization schemes, which overwhelm the physical diffusive effects with artificial viscosity. As a result of these deficiencies, no reliable conclusions can be made about turbulence model performance for this class of problems. Nonetheless, turbulence models are typically blamed for most, if not all, of the discrepancies between predicted and measured results.

3 Computational Methodology

3.1 Simulation Hierarchy. Two companion papers documented by Butkiewicz et al. (1995) and Walters et al. (1995) identified the four issues critical to the success of a computational prediction and prescribed a simulation hierarchy based on these issues. They are: (1) computational model of the physical problem; (2) accurate geometry representation and high-quality grid generation; (3) higher-order discretization scheme; and (4) effective turbulence modeling. Using a two-dimensional test case, the authors showed that the practice of applying boundary conditions in complex regions of the flowfield results in significant errors in the solution. These observations are consistent with those recently reported by Garg and Gaugler (1997). For jet-in-crossflow problems, this is particularly true at the jet exit plane or, in the case of realistic (short) L/D ratios, at the film-hole *inlet* plane. Although this fact was demonstrated in Leylek and Zerkle (1994), recent computational studies have continued to apply improper boundary conditions in these highly complex regions. The current methodology dictates the application of boundary conditions in the supply plenum, allowing the flow conditions at the film-hole inlet and exit planes to develop realistically.

The results of Butkiewicz et al. (1995) and Walters et al. (1995) demonstrate the need for both grid quality and grid refinement levels—in the form of grid-independent solutions— to be addressed in any accurate simulation. It is also critical that the computational geometry reflect exactly the physical geometry of the problem being addressed. The current methodology depends on accurate geometry and grid generation using unstructured/adaptive gridding techniques, which are discussed in more detail below.

It has been well established that for equivalent grids, higher-order discretization schemes will introduce less numerical diffusion and yield more accurate results than lower-order schemes. It is also well known that lower-order schemes require finer grid densities to achieve grid independent solutions. Each of these was shown to be true for a two-dimensional jet-in-crossflow in Walters et al. (1995). However, it was also found that even for equivalent grid-independent solutions, the first-order discretization scheme did not resolve the finer details of the flowfield as well as the second-order scheme. In addition, the second-order scheme computed more accurate surface flux results when used in combination with wall functions. For these reasons the current three-dimensional methodology prescribes a second-order discretization scheme for all simulations.

Turbulence modeling presents the final difficulty in obtaining accurate computational results. Typically, this issue represents a trade-off between computational intensity and accuracy. The majority of past simulations have used either algebraic models, such as the Baldwin–Lomax model, or two-equation models with wall functions such as the high-Reynolds-number $k-\epsilon$ model. Unfortunately, erroneous conclusions have been drawn regarding turbulence model performance based on an ineffective treatment of the previous three issues. One of the strengths of the current methodology is that accurate treatment of the computational model, geometry/grid generation, and discretization scheme allows a true judgment to be made about the performance of the combination of turbulence model and near wall treatment. For example, Butkiewicz et al. (1995) and Walters et al. (1995) found that for two-dimensional normal jets, the reattachment length is overpredicted slightly using a standard $k-\epsilon$ turbulence model with wall function when the current methodology is followed. This is contrary to results that are typically reported in the open literature, in which the $k-\epsilon$ model is usually blamed for *under*predicting the reattachment length by 10 to 20 percent.

3.2 Unstructured/Adaptive Gridding Procedure. The complex geometries associated with film-cooling applications have created difficulties in accurate geometry and grid generation in past simulations. This has led to such practices as approximating round jets as square or as equivalent area stair-step regions, or of limiting simulations to unrealistic geometries, such as discrete normal jet cases. The use of structured gridding procedures has also limited the degree to which both high grid quality (orthogonality, low aspect ratio, and low stretching ratio) and grid refinement could be maintained. Unstructured gridding techniques provide an effective means of accurately representing a given flow geometry while maintaining both refinement and grid quality (in terms of cell skewness) in high gradient regions of the flowfield. Walters et al. (1995) documented these techniques for two-dimensional situations. For complex three-dimensional geometries, it is possible that unstructured gridding techniques may offer the only method of effectively reducing grid-based errors in the solution.

The current methodology also takes advantage of the solution-based adaption features of the unstructured/adaptive procedure. This feature allows grid independence to be established more quickly and with less effort than is typically required with structured grid methods, as well as ensuring that cell concentration levels are maximized in those regions of the flowfield with the highest gradients. Care must be taken, however, to ensure that grid quality is maintained in any final mesh, and this issue is addressed in section 5.2.

4 Present Contributions

This paper documents the results of fully elliptic Reynolds-averaged Navier–Stokes computations for the case of a row of three-dimensional round jets with streamwise injection on a flat surface. The study was primarily motivated by the desire to obtain truly predictive capability for film-cooling problems using currently available technology. Key aspects of the simulation include:

- Application of the systematic computational methodology discussed in Section 2. For the first time in the open literature, a computational film-cooling simulation is truly limited by the performance of the turbulence model and near wall treatment.
- The use of state-of-the-art solid modeling for geometry and unstructured/adaptive grid generation techniques that have yet to be documented for this class of problems.
- Three-way comparison between experimental data and a previously documented structured grid simulation of an identical test case.
- Identification of probable sources of discrepancy between predicted and measured results, including computational *and* experimental errors, as well as recommendations for treating these discrepancies in future work.

5 Test Case: Three-Dimensional Streamwise Injected Jet

The three-dimensional validation test case is based on the experimental work of Pietzryk et al. (1988, 1990) and Sinha et al. (1991). The authors documented flowfield and adiabatic effectiveness measurements for a single row of holes on a flat surface, with a 35 deg streamwise injection angle and a film-hole pitch-to-diameter ratio of 3. The experimental setup is
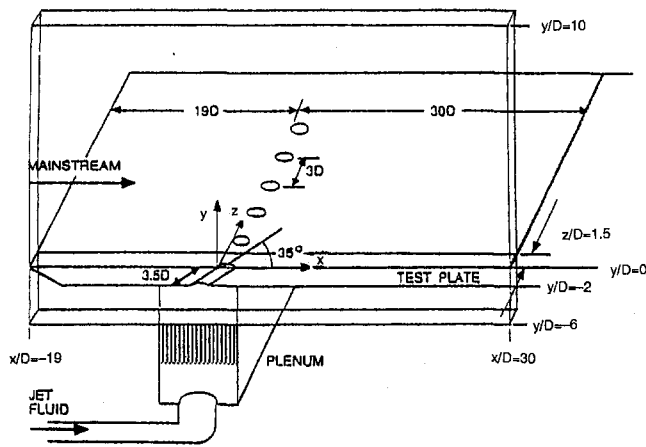
Fig. 1 Schematic of experimental test section and overall computational domain highlights the use of a supply plenum to model realistic L/D ratios

shown in Fig. 1. The film-hole diameter was 12.7 mm. The row of holes was located 19 diameters ($19D$) downstream of the flat plate leading edge, with measurements obtained from $1D$ upstream of the film holes to $30D$ downstream. The oncoming boundary layer was suctioned at the leading edge of the test surface, allowing a new boundary layer to develop upstream of the film holes. This boundary layer was experimentally determined to be fully turbulent from the leading edge onward.

The coolant fluid was injected from a supply plenum located beneath the test section, as shown in Fig. 1. Density ratio was controlled by varying the temperature of the coolant while maintaining the crossflow temperature at 302 K. The authors documented that coolant mass flow rates were equal for each of the film holes on a given test section.

Two series of measurements were performed. The first, documented in Pietzryk et al. (1988, 1990), used a length-to-diameter ratio of 3.5, with detailed measurements obtained for velocity and turbulence quantities throughout the flowfield. Density ratios of 1.0 and 2.0 were examined, with blowing ratios from 0.25 to 1.0. The second series, described in Sinha et al. (1991), used $L/D = 1.75$ and documented the downstream adiabatic effectiveness results, both along the centerline and at varying lateral locations. The density ratios examined ranged from 1.2 to 2.0, and blowing ratios ranged from 0.25 to 1.0. One important observation made at the time of the experiments involved a skewing of the coolant jets downstream of the film hole (Crawford, 1992, 1995). This fact was found to be significant when comparing predicted and measured results, and is discussed in more detail in section 7.1.3.

6 Details of Numerical Simulation

6.1 Approach. The computational model for this case matched the experimental test case, and was identical to the model used by Leylek and Zerkle (1994) for their structured grid simulation of a row of holes on a flat surface. The computational domain included the region of influence for a single film hole within the row, as shown in Fig. 1. The assumption of flow symmetry allowed a $\frac{1}{2}$ pitch extent in the lateral direction to be used to model the row of film holes. The key aspect of the model was the application of the coolant boundary condition within the supply plenum, instead of in the highly complex film-hole inlet or exit regions. The computational extent in the y direction was $10D$, which was far enough from the near-field region that a symmetry condition could be applied without significantly affecting the flowfield created by the jet-in-crossflow interaction. Velocity at the crossflow inlet was a uniform 20 m/s, with inlet temperature of 302 K. The plenum inlet

velocity was varied so that the proper blowing ratio was maintained. For all computational cases, coolant inlet temperature was 153 K, corresponding to a density ratio of approximately 2.0. At both the crossflow and plenum inlet, turbulence intensity was 2 percent, and the length scale was taken as $\frac{1}{10}$th of the inlet extent in the y direction (crossflow) or x direction (plenum). All walls were adiabatic.

The simulation was performed using the RAMPANT software package from Fluent, Inc. Extensive in-house validation has been performed for the code including laminar flow over a cylinder, turbulent flow over a flat plate, and the two-dimensional jet-in-crossflow simulations documented in Walters et al. (1995) and Hyams et al. (1996). The solver uses the fully elliptic, explicit, time-marching procedure documented in Jameson et al. (1981), on a multiblock unstructured/adaptive mesh to solve the Reynolds-averaged form of the Navier–Stokes equations. The extension of the time-marching procedure to incompressible flowfields is accomplished through the use of artificial compressibility. The simulation used local time stepping, implicit residual smoothing, and multigrid techniques to accelerate convergence to the steady state. Note that the simulation was not time accurate, but only used the time stepping scheme to achieve a final steady-state solution. The current study did not attempt to determine the effects of unsteadiness on the problem, but instead assumed a steady flowfield. Discretization of the governing equations was performed using the second-order accurate linear reconstruction approach with the flux-difference splitting scheme of Roe (1986). Details of the solution procedure and discretization scheme are available in the RAMPANT User's Guide (1993).

Turbulence modeling for the problem used the standard $k-\epsilon$ model of Launder and Spalding (1974). Near-wall quantities were calculated using the generalized wall functions available in RAMPANT. The combination of standard $k-\epsilon$ with wall functions represents what is currently the standard approach to this class of problems. By minimizing sources of error due to computational modeling, grid generation and discretization scheme, the performance of the standard $k-\epsilon$ model with wall functions can accurately be determined in the present simulation. Neither the turbulence models nor the wall functions were adjusted in any way to provide better agreement with experimental data.

Computational simulations were carried out on the South Carolina Intel Paragon machine with 64 parallel central processing units. Convergence was determined based on solution steadiness as well as overall mass and energy imbalances of less than 0.01 percent. All residual levels were reduced approximately three orders of magnitude depending on the initialization. Convergence of a typical 200,000 cell case was achieved after approximately 2000 iterations on 24 processors, with a wall-clock run time of approximately one full day.

6.2 Three-Dimensional Geometry and Grid Generation. This section details the procedure by which the high-quality three-dimensional unstructured mesh used in all of the present simulations was generated. The final grid was produced in an iterative manner using two computational tools: (1) I-DEAS Solid Modeling and Finite Element Analysis software from Structural Dynamics Research Corporation; and (2) T-Grid mesh generator available in the RAMPANT software package from Fluent, Inc.

Initially, the solid modeling capability available in I-DEAS was used to obtain an accurate representation of the flow geometry, including the cylindrical film-hole and the "elliptic breakout" into the crossflow and plenum regions. The I-DEAS two-dimensional mesh generation feature was then used to generate a high-quality triangular surface mesh for the model. The surface mesh maintained the highest levels of cell concentration in the critical regions, including downstream of the jet exit and within the film-hole. The surface mesh also used a uniform
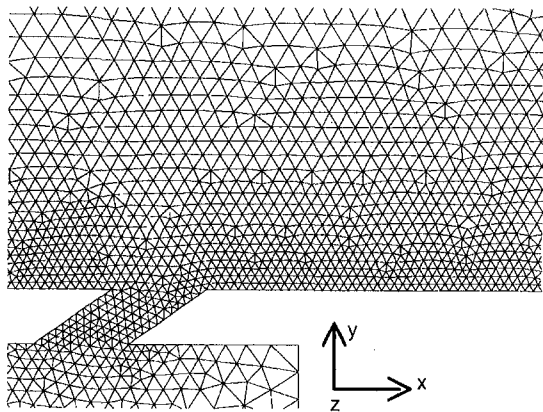
Fig. 2 Close-up of the initial grid on the centerline plane in the jet exit region shows the level of refinement in this critical region

Fig. 3 Velocity vectors along the centerline plane in the film-hole region shows separation and jetting of the coolant jet

layer of imbedded nodes within the mesh to maintain a constant cell layer along the bottom walls in order to control y^+ levels. Since wall functions were used to calculate near-wall quantities, it was critical that cell y^+ levels remain above 12, in order for the wall function results to be meaningful. The cells along the downstream bottom surface were initially sized to a height of 2 mm, which corresponded to an estimated y^+ of 30 along the surface. The final, converged solution in all cases maintained average y^+ levels along the downstream bottom surface of approximately 25. Figure 2 shows the surface mesh in the vicinity of the jet exit. The figure highlights the accurate representation of the film-hole/crossflow geometry, as well as the fine mesh in the critical jet exit region. The surface mesh was imported to the T-Grid mesh generator and the initial internal mesh of tetrahedrons was created using a Delauney triangulation method. A typical initial, or background, mesh contained approximately 125,000 cells.

For each geometry—$L/D = 3.5$ and $L/D = 1.75$—solutions were obtained on the initial mesh for all of the blowing ratio cases. The solution-based adaption feature in RAMPANT was used to determine the refinement level required for a grid-independent solution in each case. The grid was adapted based on gradients of pressure, velocity, temperature, turbulence kinetic energy, and turbulence dissipation rate. Grid-independent results were typically obtained after two solution based refinement operations, with meshes containing approximately 200,000 cells. Unlike single-block structured grid approaches, the unstructured/adaptive approach allows all of the cells to be placed in the active flow regions. Also, the cells are concentrated in those regions of the flow with the highest gradients. As a result, the grid level of approximately 200,000 is actually comparable to a single block structured grid with several times that number of cells.

7 Results and Discussion

7.1 Hydrodynamic Results. The present study was primarily concerned with computational prediction of adiabatic effectiveness downstream of a discrete jet-in-crossflow. Since the thermal field of a jet-in-crossflow interaction is dictated by the hydrodynamics, field results were also obtained and compared to experimental data. Results were obtained for $L/D = 3.5$, density ratio of 2.0, and blowing ratios of 0.5, 1.0, and 2.0. The computed near-field velocity vectors along the centerline plane for the case of $DR = 2.0$ and $M = 0.5$ are shown in Fig. 3. The figure highlights the existence of a low-momentum region along the downstream wall and a corresponding high momentum or jetting region along the upstream wall within the film hole. Figure 4 shows an orthogonal view of the velocity vectors in a cross-sectional plane within the film hole, at the
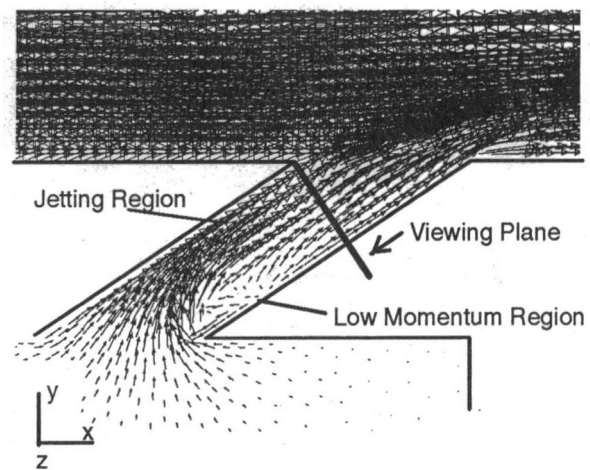
location shown in Fig. 3, exhibiting a counterrotating flow structure near the jet exit plane. Figures 3 and 4 indicate the three-dimensional swirling flow pattern within the film hole itself, a consequence of flow turning and three-dimensional separation due to the sharp-edged, inclined inlet along the downstream portion of the film hole. Note that these results are from the case of lowest blowing ratio ($M = 0.5$) and $L/D = 3.5$. As either blowing ratio increases, or film-hole length is reduced, the flow within the film hole is expected to exhibit stronger secondary motion. This is apparent in Fig. 4(b), which shows the flow at the same film-hole cross section for $L/D = 1.75$. This complex flow was first documented computationally by Leylek and Zerkle (1994), and highlights the importance of the computational model used in any jet-in-crossflow simulation. The results suggest that any accurate three-dimensional film cooling treatment must include the flow in the crossflow, film-hole, and plenum regions.
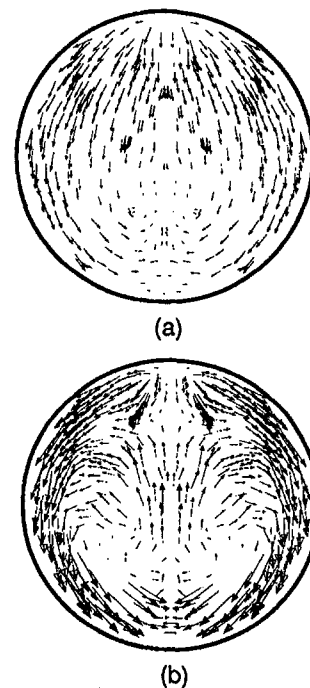

(a)

(b)

Fig. 4 Velocity vectors in a cross-sectional plane within the film hole for $L/D = 3.5$ (a) and $L/D = 1.75$ (b) show complex, counterrotating flowfield
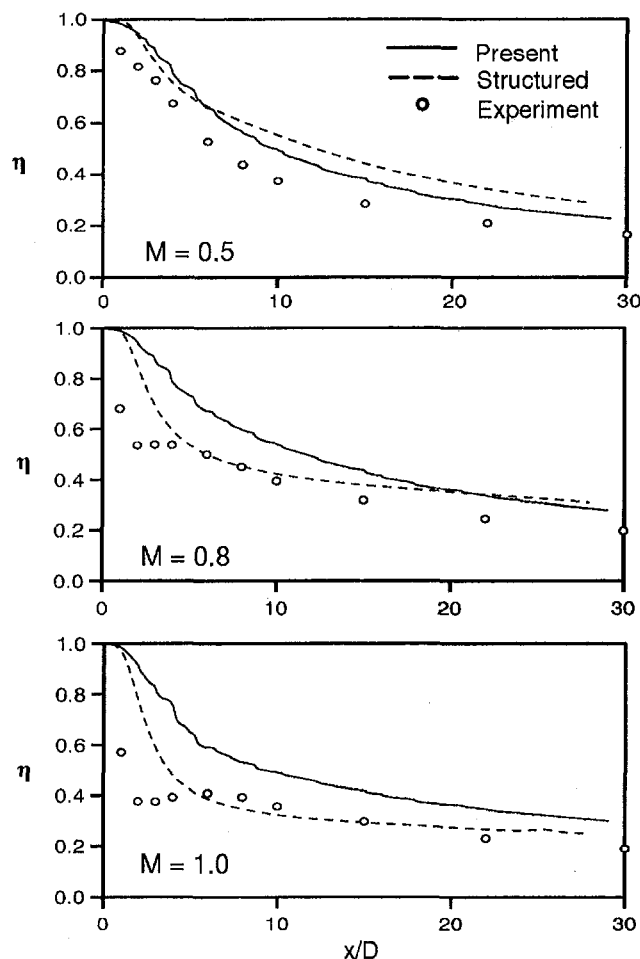
Fig. 5 Centerline adiabatic effectiveness highlights more consistent results obtained with the present computational methodology

7.2 Adiabatic Effectiveness Results. Adiabatic effectiveness results were obtained for the test case of $L/D = 1.75$, $DR = 2.0$, and M = 0.5, 0.8, and 1.0. Results were compared to experimental data documented in Sinha et al. (1991), in order to evaluate the performance of the computational methodology described above. Three comparisons are presented: centerline effectiveness versus downstream distance; laterally averaged effectiveness versus downstream distance; and lateral variation of effectiveness at various downstream locations. All of the results in this section are presented "as is." The following section (7.3) addresses possible sources of discrepancy between computational predictions and experimental measurements. When these sources are identified and corrected for, the results show improved agreement.

Figure 5 shows the adiabatic effectiveness along the jet centerline for M = 0.5, 0.8, and 1.0 respectively. Each plot contains a three-way comparison between the present unstructured/adaptive grid simulation, the structured grid results of Leylek and Zerkle (1994), and the experimental data. For all three blowing ratios, the present results show higher effectiveness along the centerline than the experimental data. This is especially true immediately downstream of the jet exit for M = 0.8 and M = 1.0. In these cases, the experiments found that the coolant jet lifts off and reattaches downstream, resulting in a sharp dip in the centerline effectiveness. Neither the present simulations nor the structured grid simulations were able to capture this detail of the flowfield, for reasons discussed in the following section. The structured grid results seem to indicate better overall agreement with the M = 0.8 and M = 1.0 data due to the sudden decrease in effectiveness immediately downstream of the jet.

However, this sudden decrease is not due to the physical mechanism of jet lift-off and reattachment, but is instead likely due to increased numerical diffusion resulting from a combination of low-order discretization scheme and a coarse, poor quality grid in this region, which is known to have influenced the structured grid results. In the region downstream of jet reattachment, the current simulation is able consistently to match the decay rate of the effectiveness, although in each case the actual levels are higher for the computation. For all cases, the structured grid results show a flatter downstream effectiveness curve than either the present computations or the experiments. This indicates that the present simulations more accurately predict the decay *rate* of the centerline effectiveness downstream than the previous, structured grid results. Since the present results show consistent trends relative to the experimental data downstream of the jet lift-off, they are judged to be more consistent than the structured grid results.

Figure 6 shows laterally averaged values of adiabatic effectiveness plotted versus downstream distance for all three blowing ratios. For M = 0.5, both the present computational results and the structured grid results show reasonably good agreement with the experiments, in general underpredicting laterally averaged effectiveness by no more than 20 percent. As blowing ratio is increased to 0.8 and 1.0, it is apparent that significant discrepancies occur immediately downstream of the jet. This is of course due to the jet lift-off and reattachment mentioned above. Downstream of the jet reattachment, however, the agreement between current predictions and experimental results is remarkably good, particularly for the case of M = 1.0. The
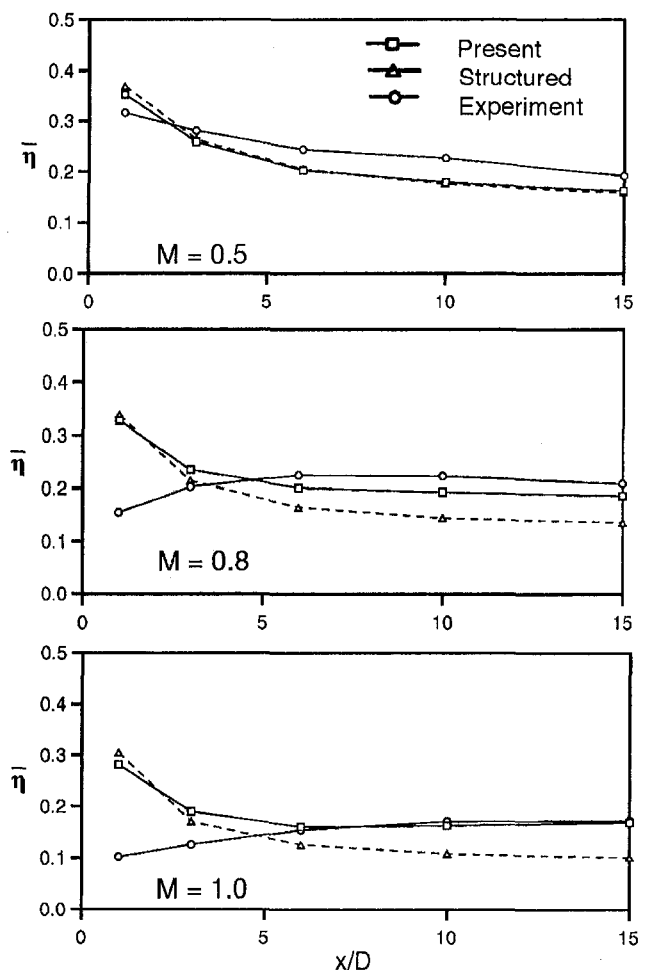

Fig. 6 Laterally averaged adiabatic effectiveness shows good agreement with experiments, particularly at higher blowing ratios
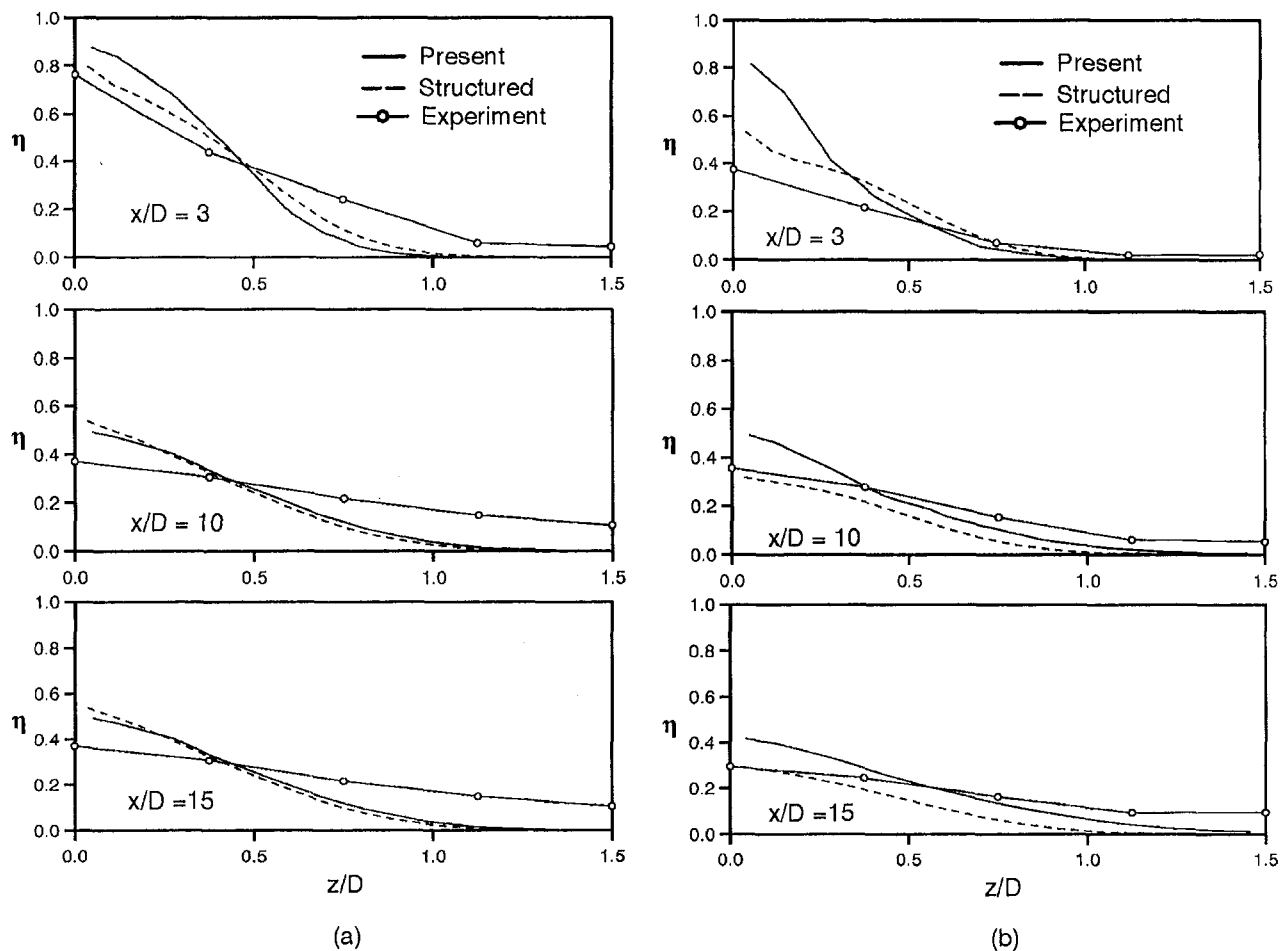
Fig. 7 Lateral variation of adiabatic effectiveness at downstream locations of 3D, 5D, and 15D for M = 0.5 (a) and M = 1.0 (b) shows underprediction of effectiveness spreading rate relative to experimental data

present results show marked improvement over the comparable structured grid results and suggest that, except for regions of lift-off that are not captured computationally, the present method does an accurate job of representing the laterally averaged effectiveness.

A key aspect of any predictive method for this class of problems is the ability to simulate accurately the lateral variation of adiabatic effectiveness downstream of the film hole. Representative plots of this lateral variation are shown in Fig. 7 for the bracketing cases of M = 0.5 and M = 1.0. Adiabatic effectiveness is plotted in the lateral (z) direction at three different downstream locations. For all cases, both the present results and the structured grid results underpredict the lateral spread rate of the effectiveness. However, it can be seen in the figure that the present results show an increase in the spreading rate over the structured grid results as the jet moves downstream. The structured grid results do indicate a sudden widening of the effectiveness band immediately downstream of the jet exit, but as mentioned above, this is likely due to numerical, and not physical, diffusion mechanisms. The figures suggest that the present methodology is more capable of representing the lateral variation than that used in Leylek and Zerkle (1994), but still underpredicts the spreading rate of the adiabatic effectiveness downstream when compared to the measurements.

7.3 Discussion of Results. Two of the cases examined, M = 0.8 and M = 1.0, were shown experimentally to exhibit jet lift-off and reattachment downstream of the film hole. This behavior was not found computationally for any of the blowing ratios. The inability of the current simulation to capture this

behavior represents a serious limitation. It is believed that the near-wall grid was too coarse to resolve this detailed feature of the flowfield accurately. The use of wall functions to obtain near-wall turbulence quantities places a restriction on the minimal cell size adjacent to a wall. For the present cases the cell sizing at the wall was 2 mm, for reasons explained in section 5.2. This cell size is rather large relative to the expected height of jet lift-off. A "proof-of-concept" simulation was performed in which the grid was refined in the near-wall region immediately downstream of the jet so that y^+ was well below the minimum levels required by the wall functions. For this case the jet lift-off and reattachment was indeed predicted. However, these results cannot be regarded as physically meaningful, since the near wall quantities could not accurately be represented with the wall functions that were implemented. The results do indicate that near-wall treatments that allow an extremely fine mesh to be used in this region will perform better than wall functions, at least at the jet exit itself. Future improvements to the simulation of this class of problems will need to include the use of two-layer or low-Re turbulence models instead of wall functions.

The results also showed discrepancies farther downstream regarding both centerline and lateral variation of adiabatic effectiveness. It is believed that the computational methodology has eliminated any sources of numerical error due to either modeling, grid, or discretization scheme in this region of the flowfield. The only sources of numerical error are likely to come from the turbulence modeling and near-wall treatment. It is known that the turbulence in jet–crossflow interactions is strongly ani-
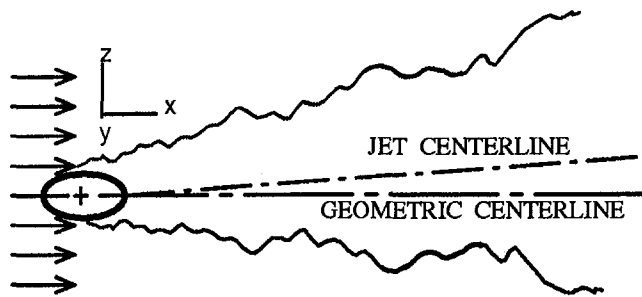
Fig. 8 Graphic depiction of jet skewness present in experimental test case. Skewness angle is exaggerated for clarity.

Fig. 10 Lateral variation of adiabatic effectiveness at x/D = 15 shows better agreement with experimental data when adjusted to account for jet skewness

sotropic, while the standard $k-\epsilon$ turbulence model is inherently isotropic. Past simulations documented in the open literature have in fact placed the blame for poor performance exclusively on the $k-\epsilon$ model. Before assessing the turbulence model performance, however, it is helpful to identify possible sources of discrepancy arising from the experimental data itself.

One likely source of discrepancy is due to a slight skewness in the jet trajectory observed at the time of the experiments (Crawford, 1992, 1995). This skewness had the effect of misaligning the geometric centerline and the actual jet centerline, as shown in Fig. 8. Experimental results for centerline effectiveness were presented based on measurements along the geometric centerline. Experimental results for lateral variation of adiabatic effectiveness were obtained using an average of both sides of the geometric centerline. In order to demonstrate the sensitivity of the results to tiny amounts of skewness, the computational results were corrected consistent with the experimental technique, using a nominal skew angle of 1.5 deg. Corrected centerline effectiveness is shown in Fig. 9 for M = 0.5 and M = 1.0. As expected, the corrected, "off-centerline" values are lower than the uncorrected values, and closer to the experimental results. Figure 10 shows the corrected lateral variation of adiabatic effectiveness for M = 0.5 and M = 1.0 at a downstream location of x/d = 15. The corrected curves are flatter, and show significantly better agreement with the experimental data. Both of these figures suggest that the jet "skewness" in the experiments
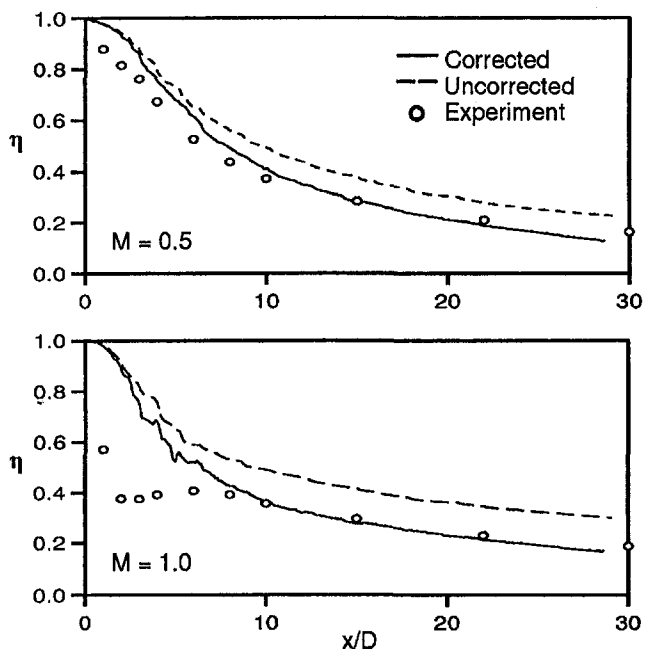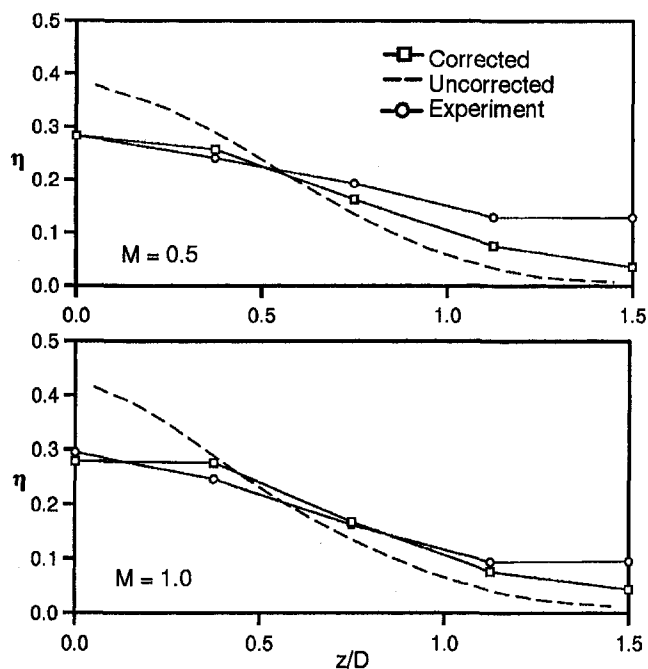

Fig. 9 Centerline adiabatic effectiveness adjusted to account for experimental jet skewness shows improved agreement with measured data

may introduce some discrepancy in the results. It should be noted that the skewness angle of 1.5 deg is based on a rough estimate made from observations of the experiments, and should not be considered as an exact correction. However, the adjusted results do indicate that the current simulations may in fact do a better job of predicting both centerline and lateral variation of adiabatic effectiveness than what is suggested in Figs. 5–7. It is worth noting that the predicted result that most closely matches the experimental data in the downstream region is laterally averaged effectiveness. This is also the result that is least likely to be influenced by a slightly skewed jet trajectory.

The authors believe that turbulence anisotropy is still a serious issue to be resolved in the simulation of film-cooling problems, especially regarding lateral spreading of the coolant jet. However, it is also clear that more code validation quality data are needed to establish the true limitations of the existing turbulence models.

8 Conclusions

A systematic computational methodology has been applied to a three-dimensional jet-in-crossflow problem typical of a realistic film-cooling application. The methodology reduces errors by addressing each of the four critical issues in a computational simulation: computational model of the physical problem, geometry and grid generation, discretization scheme, and turbulence models. Results were compared to high quality experimental data and a previously documented structured grid simulation in order to highlight the present methodology. The following specific conclusions are drawn from the study:

- The present methodology resulted in more consistent agreement with experimental data than the previous structured grid simulation documented in Leylek and Zerkle (1994). This is due to a minimization of numerical errors by a high-quality, unstructured/adaptive grid generation procedure in combination with a second-order discretization scheme.
- Downstream of the film hole, computational results tended to show higher centerline effectiveness values and

less lateral spreading of the effectiveness than the experimental results. This may be due in some part to a skewed exit condition in the experiments. Corrected computational values indicate that the data presented represents a "worst case" scenario, and in fact may do a better job of predicting downstream effectiveness levels when experimental errors are accounted for.

- The computational methodology presented has brought this class of problems to the limits of the technology that is currently readily available. The study highlights the areas of turbulence modeling and near-wall treatment that need to be improved. In particular, the use of low-Re or two-layer models that do not restrict the near-wall cell sizing and allow accurate capture of jet lift-off and reattachment at elevated blowing ratios. Also, it is likely that turbulence models that accurately represent anisotropic turbulence will be needed finally to resolve downstream characteristics, particularly the lateral spreading of the coolant jet.

Acknowledgments

References

Andreopoulos, J., and Rodi, W., 1984, "Experimental Investigation of Jets in a Crossflow," *Journal of Fluid Mechanics,* Vol. 138, pp. 92–127.

Bergeles, G., Gosman, A. D., and Launder, B. E., 1976, "The Near-Field Character of a Jet Discharged Normal to a Main Stream," ASME *Journal of Heat Transfer,* Vol. 107, pp. 373–378.

Bergeles, G., Gosman, A. D., and Launder, B. E., 1977, "The Near-Field Character of a Jet Discharged Through a Wall at 30° to a Mainstream," *AIAA Journal,* Vol. 14, pp. 499–504.

Bergeles, G., Gosman, A. D., and Launder, B. E., 1978, "The Turbulent Jet in a Cross Stream at Low Injection Rates: A Three-Dimensional Numerical Treatment," *Numerical Heat Transfer,* Vol. 1, pp. 217–242.

Butkiewicz, J. J., Walters, D. K., McGovern, K. T., and Leylek, J. H., 1995, "A Systematic Computational Methodology Applied to a Jet-in-Crossflow; Part 1: Structured Grid Approach," presented at the ASME Winter Annual Meeting, San Francisco, CA, Nov. 12–17.

Crawford, M. E., 1992, 1995, personal communications.

Dawes, W. N., 1991, "The Development of a Solution-Adaptive Three-Dimensional Navier–Stokes Solver for Turbomachinery," presented at AIAA/ASME/SAE/ASEE 27th Joint Propulsion Conference, Sacramento, CA.

Demuren, A. O., 1982, "Numerical Calculations of Steady Three-Dimensional Turbulent Jets in Cross Flow," Rep. SFB 80/T/129. Sonderforschungsbereich 80, University of Karlsruhe, Germany.

Garg, V. K., and Gaugler, R. E., 1997, "Effect of Velocity and Temperature Distribution at the Hole Exit on Film Cooling of Turbine Blades," ASME JOURNAL OF TURBOMACHINERY, Vol. 119, pp. 343–351.

Hyams, D. G., McGovern, K. T., and Leylek, J. H., 1996, "Effects of Geometry on Slot-Jet Film Cooling Performance," ASME Paper No. 96-GT-187.

Jameson, A., Schmidt, W., and Turkel, E., 1981, "Numerical Solution of the Euler Equations by Finite Volume Methods Using Runge–Kutta Time Stepping Schemes," Technical Report AIAA-81-1259, AIAA 14th Fluid and Plasma Dynamics Conference, Palo Alto, CA.

Launder, B. E., and Spalding, D. B., 1974, "The Numerical Computation of Turbulent Flows," *Computer Methods in Applied Mechanics and Engineering,* Vol. 3, pp. 269–289.

Leonard, B. P., 1979, "A Stable and Accurate Convection Modeling Procedure Based on Quadratic Upstream Interpolation," *Computer Methods in Applied Mechanics and Engineering,* Vol. 19, pp. 59–98.

Leylek, J. H., and Zerkle, R. D., 1994, "Discrete-Jet Film Cooling: A Comparison of Computational Results With Experiments," ASME JOURNAL OF TURBOMACHINERY, Vol. 113, pp. 358–368.

Patankar, S. V., 1980, *Numerical Heat Transfer and Fluid Flow,* Hemisphere Publishing Corporation, New York.

Pietrzyk, J. R., Bogard, D. G., and Crawford, M. E., 1988, "Hydrodynamic Measurements of Jets in Crossflow for Gas Turbine Film Cooling Applications," ASME Paper No. 88-GT-194.

Pietrzyk, J. R., Bogard, D. G., and Crawford, M. E., 1990, "Effects of Density Ratio on the Hydrodynamics of Film Cooling," ASME JOURNAL OF TURBOMACHINERY, Vol. 112, pp. 437–443.

RAMPANT User's Guide, 1993, Fluent Incorporated, Lebanon, NH.

Roe, P. L., 1986, "Characteristic Based Schemes for the Euler Equations," *Annual Review of Fluid Mechanics,* Vol. 18, pp. 337–365.

Sinha, A. K., Bogard, D. G., and Crawford, M. E., 1991, "Film Cooling Effectiveness Downstream of a Single Row of Holes With Variable Density Ratio," ASME JOURNAL OF TURBOMACHINERY, Vol. 113, pp. 442–449.

Walters, D. K., McGovern, K. T., Butkiewicz, J. J., and Leylek, J. H., 1995, "A Systematic Computational Methodology Applied to a Jet-in-Crossflow; Part 2: Unstructured/Adaptive Grid Approach," presented at the ASME Winter Annual Meeting, San Francisco, CA, Nov. 12–17.

Weigand, B., and Harasgama, S. P., 1994, "Computations of a Film Cooled Turbine Rotor Blade With a Non-uniform Inlet Temperature Distribution Using a Three-Dimensional Viscous Procedure," ASME Paper No. 94-GT-15.